International Journal of Precision Engineering and Manufacturing-Green Technology
https://doi.org/10.1007/s40684-024-00636-6

Online ISSN 2198-0810
Print ISSN 2288-6206

REGULAR PAPER

Utilizing Powder Bed Fusion Additive Manufacturing Technology to Fabricate Parts with Controlled Porosity and Permeability Characteristics for Filtration Applications

Seyed Haiati[1] · **Krassimir Dotchev**[1] · **Morgan Lowther**[1]

Received: 29 November 2023 / Revised: 25 April 2024 / Accepted: 30 April 2024

Abstract

Whilst the main focus of metal Additive Manufacturing (AM) aka metal 3D printing has been to produce fully dense parts; the main aim of this research is to use the technology to fabricate metallic permeable parts with controlled porosity characteristics so that they may be used as a high performance, high-pressure and cleanable and therefore "green" reusable filters for various industrial applications. The fusion bed technology, more specifically Direct Metal Printing (DMP) has been utilized to fabricate test parts with porous structure that was later tested for filtration efficiency. In DMP process, the part is built in thin layers with each layer a cross-sectional slice of the shape. This method makes it possible to design and manufacture intricate parts with detailed internal sections that is not always possible with conventional manufacturing methods. The technique also makes it possible to design and manufacture combination of solid and porous sections in one operation or in another word a complete filter assembly to be used straight off the print with no or minimal post processing required. Another advantage of using DMP is the possibility of seamlessly incorporating features like pleats to increase the filtration area, incorporate additional strengthening structures and support structures if required as well as manufacturing a graded media with larger pores on the outside getting finer as you approach the centre. The printing parameters have been selected to achieve optimum combination of tightly controlled pore size range, size distribution and mechanical strength to promote the optimum filtration efficiency and dirt-holding capacity; at the same time maintaining the structural integrity for operation under high pressures, a wide range of flow conditions, operating temperature, and compatibility with a wide range of process fluids. The results from the first round of tests on scaled down samples demonstrated that the fabricated porous metal parts are suitable to be used in a wide range of applications and operating conditions. They are bi-directional in terms of flow and as a result, they are cleanable and reusable. They can be designed to a variety of shapes and sizes with ease and are recyclable if needed. This approach of manufacturing cleanable filters can reduce the demand for new and newly processed materials. In addition, it can reduce production, distribution, and storage costs. Hence less energy usage, less pollution, and less demand for hazardous waste disposal and associated challenges with disposal and the impact on the environment.

Keywords Additive Manufacturing · Direct Metal Printing · Selective Laser Melting · Powder Bed Fusion · Filter · Permeability · Porosity · Stainless Steel

1 Introduction

Additive Manufacturing (AM) is a relatively new concept during which material is added in layers to construct a complete product. This contrasts with traditional manufacturing methods that typically involve starting with a solid block of material or casting and removing material to ultimately finish with the required shape. Great advances have been made in additive manufacturing since its inception in the 1980s. Within the general category of Direct Metal Printing (DMP) [1, 2], Direct Metal Laser Sintering (DMLS) [3,

✉ Seyed Haiati
samhaiati@gmail.com; UP112348@myport.ac.uk

Krassimir Dotchev
Krassimir.Dotchev@port.ac.uk

Morgan Lowther
morganlowther@gmail.com

[1] School of Mechanical and Design Engineering, University of Portsmouth, Anglesea Building, Anglesea Road, Portsmouth PO1 3DJ, UK

Published online: 23 September 2024

4], Selective Metal Sintering (SMS) [5, 6], and Selective Laser Melting (SLM) [5, 7–9] are three of the more familiar processes also referred to as Powder Bed Fusion subset of DMP that have gained popularity in recent years due to their flexibility and capabilities to adapt to modern manufacturing requirements. They are very similar processes, sometimes terms used interchangeably. SLM registered as a proprietary name. Many of the original patents protecting the original equipment in this area however have expired now leading to an increased number of entries to the market with new and more capable machines and the cost of the new equipment has also started to come down. In this research, DMP has been utilized to manufacture hybrid metal parts containing solid and porous volumes that would be suitable for a range of filtration applications. It is also envisaged that the concept would have applications in other industries such as aerospace, automotive, dentistry, and prosthetics [10], where porosity, mechanical strength, and lower weight are desirable attributes.

This contrasts sharply with the conventional methods of manufacturing sintered metallic filters which typically involves stretching of thin metal strands, typically stainless-steel wires to reduce the thickness while maintaining the mechanical strength and weaving the wires prior to application of heat to sinter and bond them together.

1.1 Filtration Principles

The origins of filtration date back to 500BC where sand was used to filter out contaminants in drinking water [11]. Since those days, the applications of filters across the industry have increased enormously and so have the types of filters used in various applications. Filters are used to clean and purify water and various other foods and beverages. Filters are also used in pharmacology and hospitals to capture virus and almost any other contaminants whose presence present a risk to health and equipment. Industrial applications of filters include hydraulics systems to protect equipment, systems to clean air in public places and on aircrafts and others.

There are three main capture mechanisms by which suspended solid contaminants in a fluid are separated [12]:

- Inertial impact where the momentum of the solid contaminant results in an impact and eventual separation of solids from fluid.
- Diffusional separation is where smaller solids with smaller mass hence momentum move randomly until they collide with the filter medium and come to rest.
- Direct interception, where the contaminant is captured in a web of interwoven fibrous material.

It is generally accepted that direct interception is the most effective method for separating particles from liquids, while inertial impaction and diffusional interception are more effective in gas filtration. To enhance the conventional filter's separation effectiveness, it is possible to manipulate the contaminant, fluid, or filter media system.

1.2 Possible Options for Manufacturing of Porous Media

As indicated, the aim of this research is to investigate the feasibility to manufacture a permeable metallic medium for filtration using DMP technology and a direct capture method of filtration. The following methods for the construction of a porous/ permeable media using AM technology have been considered:

- geometrically defined [13] lattice structures;
- the use of mono-size spherical particles bonded together;
- geometrically undefined (random) structures containing consistent voids to capture and remove contaminant.

An example of a lattice structure is shown in Fig. 1a. Figure 1b shows a 3D metal mesh with tubular strands.

The above methods were considered not to be the most effective due to problems associated with cleaning the unmolten particles trapped between solid sections given the pore size requirements and metal particle size range. The use of mono-size particles is purely a theoretical concept to demonstrate the possibility but in practice, it is not feasible to obtain perfect mono-size spherical metal dust and melt them in such a manner that they are all bonded tangentially and perfectly. Also, whilst using mono-sized spherical metal particles may be feasible in the production of finer grade permeable media of less than 5 μm, for the coarser filters it doesn't result in the most efficient solid volume to void volume ratio given that the radius of the largest spherical particle that fits in the gap between three identical and tightly packed spheres is given by the following equation:

$$r = (R/\cos 30) - R \tag{1}$$

where **r** is the radius of the pore, **R** the radius of the dust particle. The radius of the pore r is approximately 15% of the radius of mono-sized metal dust particles R. Figure 2 shows the relative sizes of three tightly packed spheres and the gap that the largest spherical particle will fit in. Where R is the radius of mono-size spherical metal dust and r is the radius of the largest sphere inscribed in between three tangentially touching mono-size spheres.

The preferred method however was producing permeable parts with geometrically undefined pores [14] using DMP that made it possible to achieve much smaller pore sizes that were compatible with the particle size distribution of the powder particles. In addition to the above DMP

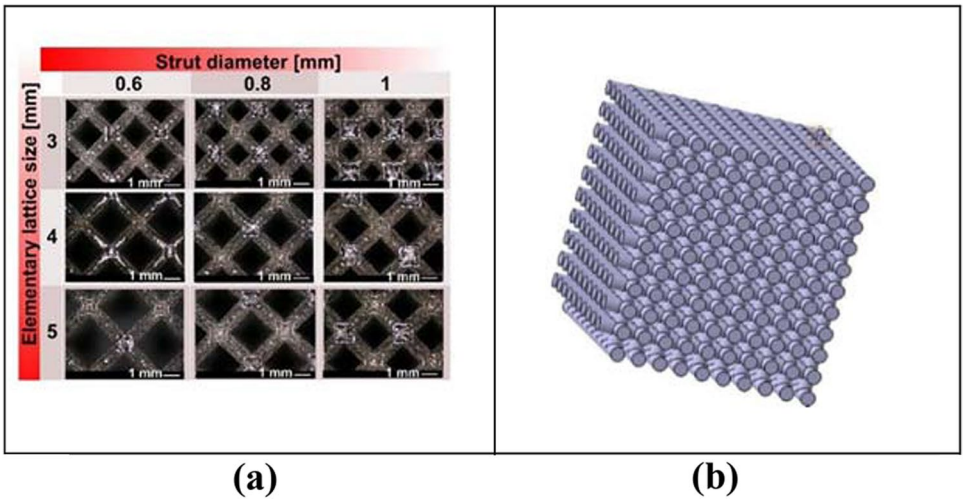

Fig. 1 **a** Lattice Structures. **b** 3D Metal Mesh

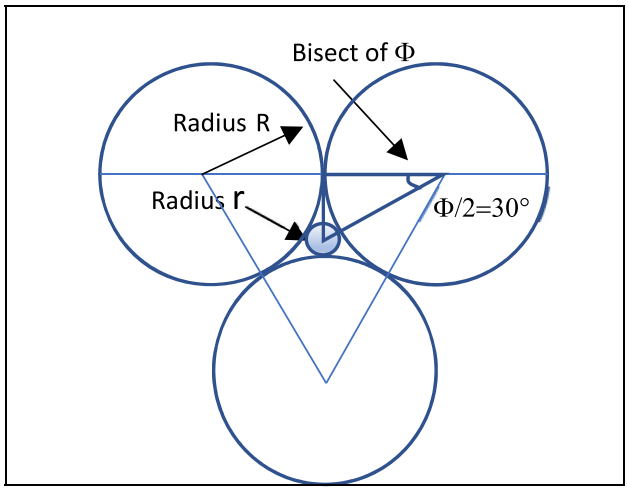

Fig. 2 The size of the largest sphere inscribed between three tightly packed spheres

manufactured parts are generally expected to have superior mechanical properties in comparison to similar parts manufactured using binder jetting technique for example. It would also be more practical to make any shape or geometry using an undefined geometry pore structure than a mesh or lattice. It would be overly complex for example to generate a curvature and maintain the pore sizes if it was required to manufacture a pleated mesh or a lattice form to increase the filtration area. Another advantage of DMP would be the seamless manufacturing of hybrid components combining solid and porous parts in one operation. The geometrically undefined method also generated higher number of smaller size pores per volume than was possible with other methods, resulting in lower clean differential pressure and longer life. To achieve the main aim of this research a number of test parts have been produced using a commercial DMP machine ProX300® [1] and then tested as described in the following sections.

1.3 Methods for Characterization of Pores in Porous Media

Conventional methods for evaluation of pore size and shape characteristics and density measurement in the majority of existing studies involve visual measurements usually SEM or optical microscope and Archimedes' method of buoyancy to establish the density. However, it is very difficult to analyse the porosity and density using the above techniques for the following reasons:

- Surface pores to be measured must be prepared and polished first particularly for optical microscope. This process may alter the shape and the size of the visible pores as demonstrated in Fig. 3.
- The pores that are irregular in their geometry cannot be measured accurately and the hidden pores or parts off cannot be measured at all.
- There is a good probability that there are hidden pores that cannot be seen, and they are difficult to quantify as a result.
- Although it may be possible to use automated imaging equipment or MRI, those techniques also encounter some of the above-mentioned issues.

With regards to using Archimedes' principle of buoyancy to establish the relative densities the following problems arise especially when a relatively heavy metal like stainless steel is used for production. Fluid accessing all the void volume and particularly partially obscured pores is not guaranteed and the relative densities of metal and the wetting fluid would make the measurement of the volume and the mass of the displaced fluid rather difficult.

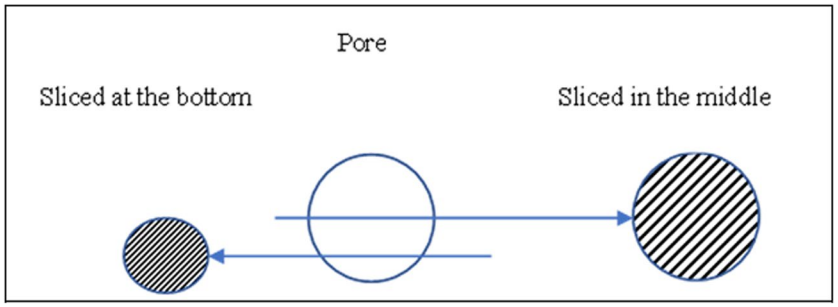

Fig. 3 Relative pore size depending on the position of the cut during surface preparation

Using relatively high surface tension liquids such as water simply adds to the wetting problem. ideally, a fluid with a low surface tension should be used to facilitate better wetting (water surface tension is 72 dynes/cm whereas IPA has a surface tension of 23.5 dynes/cm). it is also difficult to accurately measure small amounts of displaced fluid with smaller samples. To overcome the above problems a combination of Fabrication Integrity (ISO 2942) [15] and Multi-pass Test (ISO 16889) [16] was used to determine the filtration efficiency of porous/ permeable metal parts, hence establishing relative porosity and pore size characteristics.

1.4 Fabrication Integrity Test ISO 1942:2014[15]

Fabrication integrity test is an International Organisation for Standardization test protocol that involves submerging the sample under test in a fluid, usually Iso Propyl Alcohol (IPA). Air is gradually introduced into the test item with the openings sealed. The air pressure is gradually increased and measured until the first stream of bubbles starts emerging from the surface of the test article. The pressure at which the air bubbles start emerging from the surface is directly proportional to pore sizes hence permeability.

To conduct the test the filter cartridge is Immersed in the test fluid for five minutes to ensure thorough wetting. Ensuring that both ends of the element (where applicable) are sealed. The filter is positioned so that its major axis is horizontal, and the media is between 10 and 15 mm beneath the surface of the test fluid. Air pressure is slowly applied inside the submerged filter until the element's first bubble point value is reached where the first stream of bubbles starts to surface from the element and the pressure reading at this point is recorded. This is a highly effective and non-destructive way of measuring and comparing the permeability of porous media. The fabrication integrity test is primarily used as a production test of filter cartridges to determine the built quality. The test highlights the approximate rating of filter media, as well as the integrity of side seams and endcap media bonding and filtration media itself.

1.5 Multi-pass Test ISO16889: 2022[16]

Developed in the 1960's, the test aim is to simulate continuous circulation of fluid which is contaminated through the filter under test. In a multi-pass test, a dust with known particle size range and particle size distribution (ISO medium A3 test dust) suspended in the test fluid is injected in fluid that is circulating through the test article (filter) to block it to a pre-determined terminal differential pressure. Samples are taken continuously and simultaneously from upstream and downstream of the filter under test and analysed using online laser particle counters. The data is analysed, and filtration efficiency, dirt-holding capacity, and filter blockage characteristics are determined.

Due to the small size of the experimental cylindrical parts, the multi-pass test was modified to test at a flow rate of 25 mL/min by positioning the test items directly between the laser particle counters. The filtration efficiency tests were carried out in MIL-H-5606 grade mineral oil at 15 cSt. viscosity. The tests ran for at least one hour and the results were analysed.

The information typically recorded during a multi-pass test is differential pressure measurement; upstream and downstream particle counts; flow rate; temperature and the weight of test contaminant added to the system at regular intervals throughout the test. Typical result outputs may include upstream and downstream particle counts; beta-ratio against particle size; particle size where beta ratio typically is 2, 10,100,1000 and 2000; test element differential pressure against weight of test contaminant added (dirt loading curve).

1.6 Review of Current Similar Products[17–20]

Porous metal filters and membranes have become increasingly popular due to their durability, stability and compatibility with a wide range of chemicals. They can generally be used at higher temperatures and have superior mechanical strength. They are made using a wide range of metals and metallic alloys. Various production methods are used in the production of metallic filters from traditional woven metal mesh to sintered metal powders and 3D metal printing. The range includes

geometrically defined structures such as metal mesh, lattice structure and geometrically undefined pore structure such as sintered metal powder. It is not uncommon to come across traditionally manufactured pleated metallic mesh filters using a single layer of metal mesh. The sintered type either additively manufactured using Binder jetting technique or metal powder sintered constructed filters tend to be plain cylindrical.

The advantages of using DMP to manufacture geometrically undefined porous metal filters as defined in this article are as follows:

- Features like pleats to increase surface area, additional strengthening structures, support rings and other features can be seamlessly added.
- Scaling up or down the size of the parts is simple relative to the complex geometries involved in creating pleats and round edges whilst maintaining a consistent pore size in the case of a lattice structure for example.
- Solid parts, shells and capsules can be incorporated into the design to produce an assembly in one operation.
- Additional features like graded pore structure or pore size variations can be achieved consistently by controlling the printing parameters to achieve larger pores getting finer going from upstream to downstream for enhanced efficiency.

2 Printing of Porous Test Parts

DMP generates a solid part by adding thin layers of fine metal powder and bonding them together by means of a laser source. The most influential parameters that control the construction of metal parts, also common to all 3D metal printers, that have a direct effect on the mechanical strength, surface finish, and density of the finished parts are *laser power, hatch distance, layer thickness, and scanning speed*.

In ProX300 DMP machine (3D Systems), used in this study, the laser power is delivered via a 500W fibre laser of 1070 nm wavelength on the powder bed surface. It melts the particles and bonds them together layer by layer. The melting is normally deeper than the layer thickness to bond two subsequent layers. Hatch distance (aka scan space) is the distance between two subsequent laser scan paths and, scanning speed which is the speed of the laser beam across the current part section in X or Y axes. Layer thickness is the thickness of the layers of powder delivered to the printing chamber. Depending on the required speed, resolution, and powder particle size it can be changed to a higher value. It was set to 0.04 mm for these experiments. The scan speed is the linear speed of the laser beam. The mathematical relationship between the Volumetric Energy Density (VED) and the above parameters is given in the Eq. 2 below, also used to calculate the volumetric energy density in Tables 2, 5, 8, and 9:

$$\mathrm{VED} = \mathrm{LP}/\left(\mathrm{SS}^{*}\mathrm{HD}^{*}\mathrm{LT}\right) \tag{2}$$

where VED is the volumetric energy density in J/mm^3; LP—is the laser power delivered to the powder bed in W; SS – is the laser scanning speed in mm/s; HD – is hatch distance in mm; and LT – is the layer thickness in mm.

The recommended values of the above parameters to fabricate a fully dense part are: laser power: 150W; scanning speed: 1200 mm/s; sack-and-forth scan strategy; hatch spacing: 70 µm, and layer thickness of 40 µm. Also, the fabrication take place in a Nitrogen (N_2) gas-backfilled build chamber. The key factor when manufacturing porous structures is to ensure sufficient VED in order to maintain the mechanical properties hence structural integrity and at the same time stop short of totally melting the metal powder to make a fully dense part.

2.1 Selection of DMP Printing Parameters

For the fabrication of the test parts, a commercial ProX300® DMP machine, manufactured by 3D Systems [1], loaded with nitrogen gas atomized 17–4 PH Stainless steel pre-alloyed powder called LaserForm 17-4PH [21], was used. This type of metal powder is widely used in aerospace, petrochemical, and chemical applications because of its corrosion resistance and good mechanical properties. The composition of this metal powder is given in Table 1.

2.1.1 The Manufacturing of the Cylindrical Test Samples

Test samples with various parameter combinations have been printed to test the feasibility of this approach. The sample geometry was a cylindrical model with a 25 mm outer diameter, 30 mm height, a wall thickness of 3 mm, and closed at the base. The plan was to produce 16 porous parts and one solid cylinder as a reference. The printing was initiated with the Prox 300 DMP recommended printing parameters for making a solid reference part. This was followed by a series of porous parts in increasing levels of porosity to establish the most appropriate span of parameters to generate optimum parts in terms of compromises between porosity, dirt capacity and structural integrity. There ProX 300 DMP machine has over one hundred printing parameters to select from. The most important of those

Table 1 17–4 PH Stainless steel powder chemical composition and % by weight

Element	Fe	Chromium Cr	Nickel Ni	Copper Cu	Silicon Si	Manganese Mn	Niobium + Ta (Nb)
Weight, %	Bal	15–17.5	3–5	3–5	< 1	< 1	0.15–0.45

Table 2 The printer parameters for production of the first batch of 16 scaled-down cylindrical test parts

Sample	Laser Power (W)	Scan Speed (mm/s)	Hatch distance (μm)	Layer thickness (μm)	Lin Ed (J/mm)	Area Ed (J/mm^2)	Vol Ed (J/mm^3)
1	120	1200	70	40	0.10	1.43	35.71
2	120	1200	100	40	0.10	1.00	25.00
3	120	1200	130	40	0.10	0.77	19.23
4	120	1200	160	40	0.10	0.63	15.63
5	100	1200	70	40	0.08	1.19	29.76
6	100	1200	100	40	0.08	0.83	20.83
7	100	1200	130	40	0.08	0.64	16.03
8	100	1200	160	40	0.08	0.52	13.02
9	80	1200	70	40	0.07	0.95	23.81
10	80	1200	100	40	0.07	0.67	16.67
11	80	1200	130	40	0.07	0.51	12.82
12	80	1200	160	40	0.07	0.42	10.42
13	60	1200	70	40	0.05	0.71	17.86
14	60	1200	100	40	0.05	0.50	12.50
15	60	1200	130	40	0.05	0.38	9.62
16	60	1200	160	40	0.05	0.31	7.81
*Solid	150	1200	50	40	0.13	2.50	62.50

*ProX 300DMP recommended parameters for fully dense part

parameters are as mentioned previously, laser power, scanning speed, hatch distance and the layer thickness which determine the energy density hence control the melting of metal powder. Initially those parameters were selected using data from a series of experiments to cover the full range from solid to very porous. This was achieved successfully and provided a very good indication of the most suitable range of energy density to produce the best combination of porosity and mechanical strength. The data however due to time and resources constraints is limited at this stage. Over time and with the production of more parts followed by more testing and gathering of all the relevant information, a growing database will eventually be available to aid with the design and manufacturing of parts for with enhanced precision. The selected sets of laser parameters to print the cylindrical parts are shown in Table 2. To intentionally increase the porosity of the manufactured parts the parameters were selected so that the energy density was reduced in the range of 12.5% to 57.14% of default printer parameters values for making a fully dense part.

A test batch of seventeen samples of the same part was printed in one build. Only 7 out of 17 printed samples were successfully manufactured. The rest failed to print due to insufficient energy density. They were too fragile to be removed from the printing baseplate or simply disintegrated during the removal process due to insufficient energy density. Those that survived underwent a series of tests to establish their suitability to be used as filters. The fully solid cylindrical part was not used in any of the experiments described hereafter. This experimental build was designed to establish the capabilities of the ProX 300 printer to print a part with permeable properties.

Increasing the hatch distancing from 100 to 130 μm and/or reducing the laser power from 100 to 80W resulted in the failure of samples 8 to 16. Conversely, increased laser power and/or reduced hatch distancing resulted in parts 1 and 5 being too dense and insufficiently permeable to be suitable.

The results also highlight the level of influence of laser power and hatch distancing on the properties hence the porosity of the printed parts.

2.2 Manufacturing of Pleated Samples: Increasing Effective Filtration Area and Flow Capability

Encouraged by the test results from the first series of cylindrical test samples, the next stage was to use the data to fine-tune the printing parameters and manufacture a larger part with increased surface area to perform more realistic tests.

To achieve the above objectives a new pleated design was created. The new design which was wider and longer can be seen in Fig. 4. It is 70 mm long, 40 mm outer boundary diameter with a wall thickness of 2 mm. It was pleated to increase the dirt-holding capacity and add additional structural support. This particular design consisted of 9 pleats of approximately 12 mm height. By making the wall pleated the surface area hence the effective filtration area was increased by 50%.

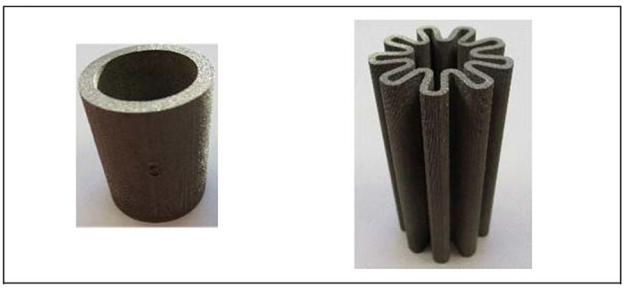

Fig. 4 The initial cylindrical part and the pleated part

Table 3 printing parameters for the new pleated samples. They show the range used to manufacture porous samples

PTS	Power (W)	Speed (mm/s)	H distance (µm)	thickness (µm)	Energy density (J/mm^3)
1V1	100	1200	80	40	26.04
2V1	100	1200	100	40	20.83
1V2	100	1200	80	40	26.04
1V4	100	1200	75	40	27.78
3V4	100	1200	85	40	24.51

Several batches of new pleated test samples (PTS) were produced with combination of DMP parameters. The most successful combinations are shown in Table 3.

2.3 Postprocessing and Cleaning of the Samples

After the printing process, the samples were separated from the substrate by means of wire electro-discharge machining (EDM). The non-molten powder was removed using a wire brush and airline.

After preliminary inspections and fabrication integrity testing of samples, there was evidence of fine metallic particles trapped within the structure of the test articles. This suggested the migration of loose metal dust through the body and the potential of particles being released into the system where the filters were being used. To ensure the total cleanliness of the parts before further examination and in particular filtration efficiency tests a cleaning procedure was implemented which is as follows:

- First, the printed samples were thoroughly cleaned mechanically by means of shaking, brushing off, and air blasting with the aid of a high-pressure airline. It is important to ensure health and safety procedures are followed and PPE is used during this procedure. Metal dust particles can present serious respiratory and other health issues.
- The components were then placed in an ultrasound bath containing a suitable solvent in this case petroleum ether for a period of at least 30 min.
- After the ultrasound, the parts were installed in a suitable test housing and subjected to a pulsating high-pressure clean air supply to dry and release the remaining contaminants in both directions, in–out and out-in.

2.4 SEM, EDS, X-Ray, and Optical Microscope Analysis

Although SEM and optical microscope imagery are commonly used for evaluation of porosity, in this report they are used as an aid to visually examine the variation with varying levels of printing volumetric density. The primary method for evaluation of porous parts performance as a filter medium was industry standard filtration tests fabrication integrity and multi-pass. In addition, several other techniques were used to get a better understanding of the internal structure that was fabricated via DMP such as:

- SEM: A Hitachi TM3000 tabletop microscope SEM/EDS system was used to capture the detailed images of the cylindrical part structure.
- X-Ray: X-ray images of the raw (unpolished) cylindrical sample 6 (Table 2). A Nikon XTEX XT H225 CT system for inspection of cylindrical parts was used. The software used for processing X-ray images was VG Studio MAX.20.
- Optical Microscope: Optical microscope images of the polished cross-section surface cylindrical samples 5 and 6 (Table 2). For this, an Olympus BX40 clinical microscope was used.

3 Test Results

After the production of porous cylindrical test parts, SEM and X-ray imaging was carried out on selected samples. The examination under an Optical microscope followed a series of industry-standard tests designed to establish the filtration performance of hydraulic filters. Cylindrical samples 5 and 6 (Table 2) were cut up after performance tests and prepared for examination under an optical microscope (Fig. 5).

3.1 SEM

The more fragile sample 8 (Table 2) that would break up quite easily was used for SEM and EDM analysis as shown in Fig. 6a, b, and c.

The SEM images of sample 8 show in detail the structure and the size of pores. Figure 6a shows the top surface of the cylindrical part sample 8 in the X–Y plane. Figure 6b

Fig. 5 Polished sections from the cylindrical samples

is the underside of (a) broken off the main body rather than cut with a cutting tool to avoid disturbing or deforming the structure. Figure 6c and d are SEM images of the side view, plane Y–Z. They show all the metal particles have melted and fused together however, the structure is quite weak borne out by the fact that pieces were broken off the main body without tools or much effort.

3.2 X-Ray Imaging

The X-ray images of part 6 generally show a uniformity of the structure and integrity throughout without obvious signs of defects. There is a slight indication of a higher concentration of porosity towards the inner diameter of the cylindrical part. The X-ray did not highlight any unexpected irregularity, large gaps, or cracks in the structure. This was also confirmed by the filtration performance test later.

Figure 7a and b show a cross section (a) and enlarged cross-section (b) in more detail.

3.3 Optical Microscope Images of the Polished Cross-section Surfaces (Cylindrical Samples 5 and 6, Table 2)

The optical microscope images were obtained to observe the influence of varying the volumetric energy density by changing the hatch distance and the resultant degree of porosity in the structure.

The SEM images, Optical microscope images and the X-ray images all show the corelation between the energy density and porosity. This was later confirmed also by filtration efficiency tests. Also apparent was the consistency and repeatability of the printing process.

Figure 8 demonstrate optical microscope images of parts 5&6. Figure 8a and b cut vertically, Fig. 8c and d cross-section of polished surfaces of the cylindrical samples 5 and 6.

These images suggest consistency of the porous structure in vertical and horizontal planes and throughout the structure.

3.4 Fabrication Integrity Testing: Cylindrical Samples

The first series of tests on cylindrical samples was the fabrication integrity test in accordance with ISO 2942 [15] to measure the permeability of the manufactured samples. The

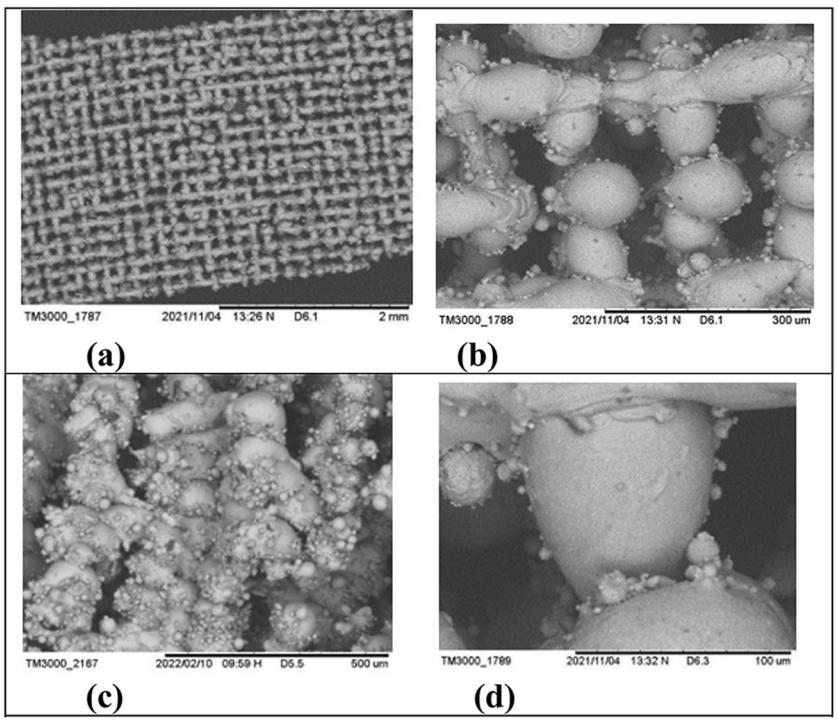

Fig. 6 **a** SEM images of: Top surface of the cylindrical sample 8 x–y plane. **b** Sample 8 structure in the x–y plane. **c** sample 8 in y–z plane. **d** sample 8 y-x in more detail

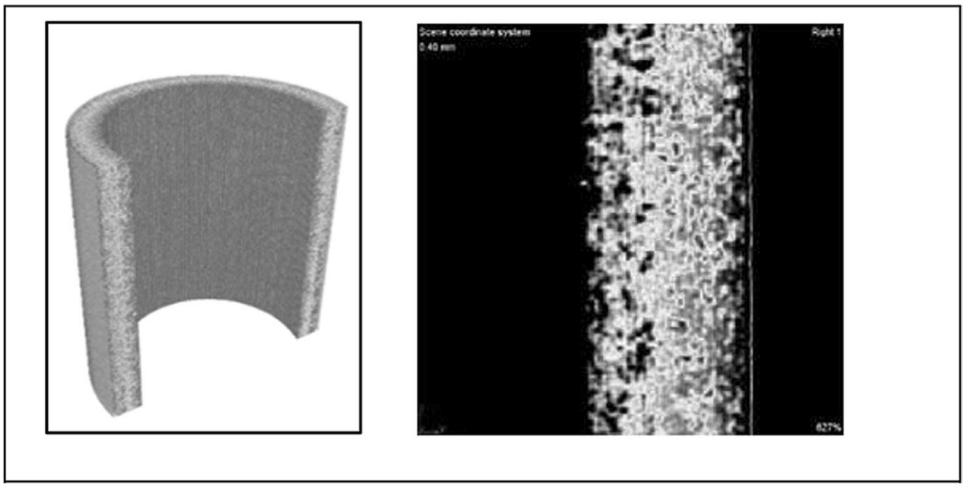

Fig. 7 **a** and **b** are X-ray images of the cylindrical sample 6

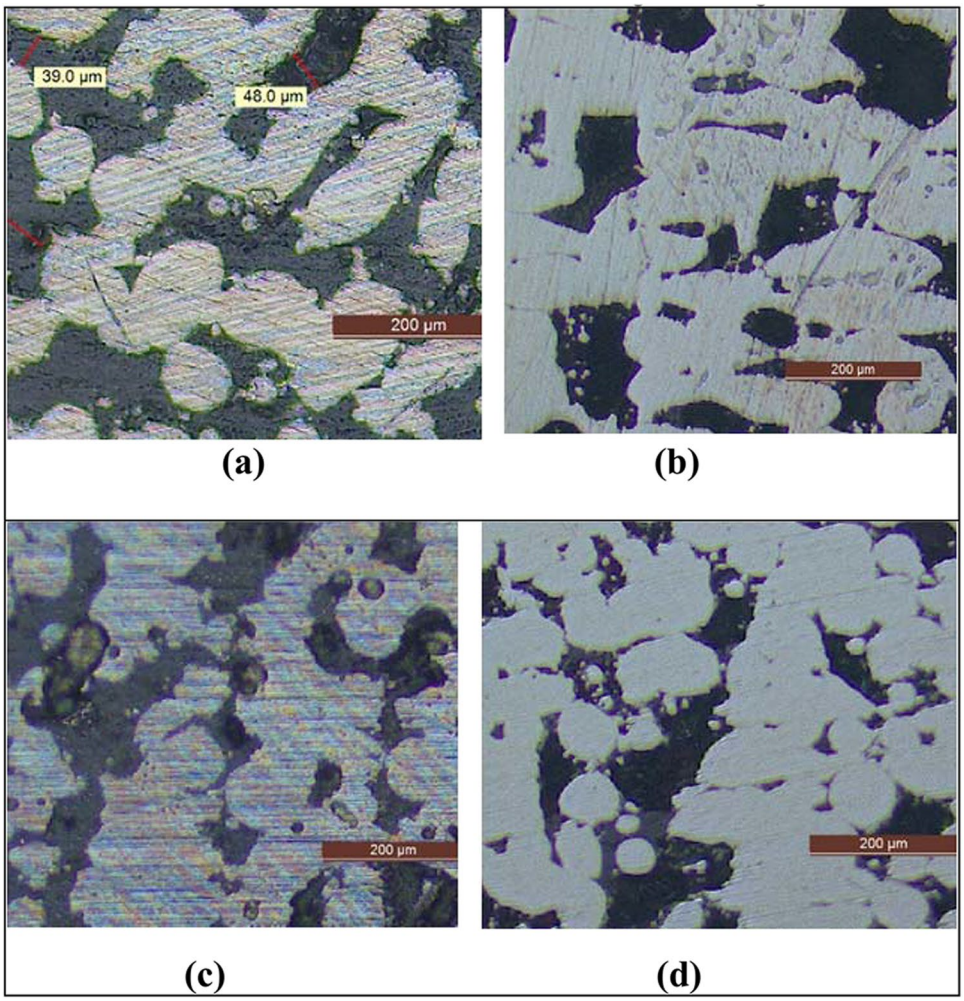

Fig. 8 Optical microscope images of polished cross-sections of cylindrical sample: **a** sample 6 (middle horizontal section). **b** sample 5 (middle horizontal section). **c** Cylindrical sample 6 (vertical section). **d** Cylindrical sample 5 (vertical section)

measurements are of pressure expressed in inches of water gauge ("WG) for the first, second and third bubbles emerging from the top of the submerged samples in IPA. There is usually a very good corelation between the bubble test values and filtration characteristics of a permeable medium that makes this test ideal as a production test (Table 4).

Table 4 Fabrication integrity test results of cylindrical samples

Bubble test results: *("WG Inches of water gauge)				
ID	1st	2nd	3rd	fizz@ 12L/min
1	25.1	26.6	28.1	No Flow
2	8.1	8.9	10.4	2 L/min > 100" WG
3	6.4	6.7	6.8	14.4
4	6.7	6.8	6.9	13.4
5	30.5	34.4	36.1	1 L/min > 100" WG
6	5.7	6.2	7.5	23.5
7	4.3	4.4	4.4	7.9

*The pressure is expressed in "Inches of Water gauge measured inside sample. 1 inch Water Gauge = 2.49 mbar

3.5 Multi-pass Filtration Efficiency Test [16]

The following selected samples, 4,6 and 7 based on bubble test results were multi-pass tested since the rest were either too dense with very high clean differential pressures or some on the other side of the spectrum were very coarse with very low bubble test values. The test flow rate was 25 ml/min for the cylindrical parts due to their small size. Due to the relatively small size therefore surface area of cylindrical samples, they were installed directly between the upstream and the downstream laser particle counting sensors. The sensors are operated at the manufacturers' recommended flow rate of 25 mL/min. The smaller flow rate also made it possible to obtain enough data for a representative statistical analysis of data. The minimum flow rate of the actual multi-pass test stand itself was 2 L/min which was the selected flow rate for testing the larger pleated samples with increased surface area and lower clean differential pressure. The flow versus differential pressure was carried out up to 3 L/min for pleated parts (Table 5).

Figure 9 below is part of a typical output report.

3.6 Fabrication Integrity Testing: Pleated Parts

Fabrication integrity tests were carried out on various batches of pleated parts. Selected samples from different batches were chosen for multi-pass tests based on their bubble test results. The pleated parts were printed in small batches together with other items for other research projects purely due to space availability of the printer. The samples details and the test results are shown in Table 6.

3.7 Multi-pass Filtration Efficiency Testing: Pleated Parts

The pleated parts were tested at 2 L/min, the minimum test stand flow rate to a terminal differential pressure of 16 bar for reporting, but the injection of contaminant was continued until the differential pressure reached 40 bar in an out-in direction. Pleated sample 1V4 was pressure tested in the reverse direction (in–out) to 30 bar before the sample was detached from the post and the test was terminated. The summary of filtration efficiency tests for pleated parts is given in Table 7.

Table 5 Cylindrical parts filtration efficiency test results

	Summary of filtration efficiency tests of cylindrical parts to 16 bar			
Sample ID	ß = 2	ß = 10	ß = 100	ß = 200
7	14	> 40	> 40	> 40
6	5.1	14.3	> 40	> 40
4	12.4	23.9	> 40	> 40
A Typical 12 µm Filter	< 4	6.6	10.1	11.2

Samples, 1V4 and 1V2 showed the best performance of 36.7 µm and 38.2 µm respectively at β = 100 or 99% efficiency. Put simply for every one hundred 36.7 µm or 38.2 µm size particle respectively only one passed through the filter.

Testing the pleated parts at 2 L/min flow rate also meant testing at forty times the flow rate for the cylindrical parts and to much higher differential pressures.

For higher flow rates and dirt holding capacities larger parts in terms of height, width and more pleats can be produced only by scaling up the original design. There is also the option of using multiple number of parts individually or in a cluster.

3.8 Differential Pressure Versus Contaminant Injected

Sample 1V4 was pressure tested to 40 bar differential in an out-in direction (Fig. 10) without any sign of collapse or deformation.

In an in–out direction, the test part which was glued to the filter housing post came off the post at 30 bar differential pressure. There was no sign of damage to the porous part itself.

Above scenario is not a situation encountered when the porous part is manufactured as an integrated part of a solid housing in a complete product design.

Pressure testing as described above in both flow directions is used to establish the actual collapse (out-in) and burst (in–out) pressure resistance of the manufactured parts.

The Differential pressure versus injected contaminant is shown in Fig. 10. This figure also shows the fairly linear relationship between the rise in the differential pressure across the filter and the weight of added contaminant. This

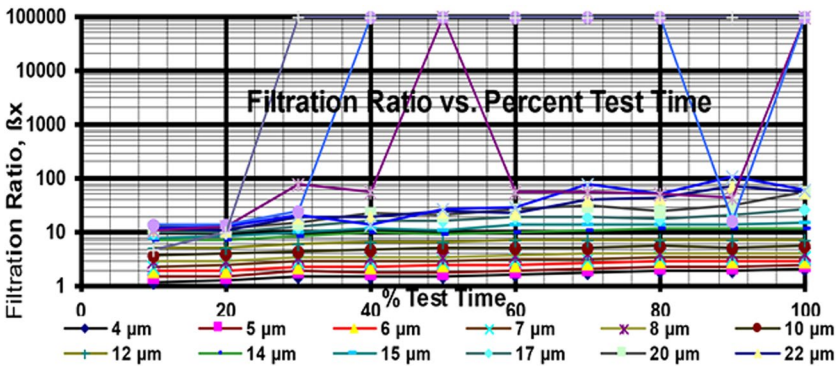

Fig. 9 Filtration ratio across 16 monitored sizes (4–40 mm) versus % time to terminal differential pressure for sample 6

Table 6 Fabrication integrity test results of the pleated samples

	Fabrication Integrity Test (Inches of water gauge WG)					
Sample ID	1st	2nd	3rd	10th	Fizz	Comment:
1V1	6.1	6.3	6.4	7.2	17.2	
2V1	5.2	5.4	5.6	5.9	8.7	
1 V2	12.3	15.2	17.5	23.9	64.9	> 5L/min
1V4	29.1	30.4	31.5	38.1	100 +	
3V4	10.1	10.5	11.4	19.1	76.4	

Table 7 Filtration efficiency results of the pleated samples. The maximum particle size monitored was 40 µm due to the calibration of the particle counters

	Summary of filtration efficiency tests to 16 bar			
Sample ID	ß = 2	ß = 10	ß = 75	ß = 100
1V1	< 4	27.5	> 40	> 40
2V1	22.5	38.5	> 40	> 40
1 V2	< 4	21.1	34.7	36.7
1V4	< 4	25.5	37.3	38.2
3V4	< 4	24.9	39.2	> 40

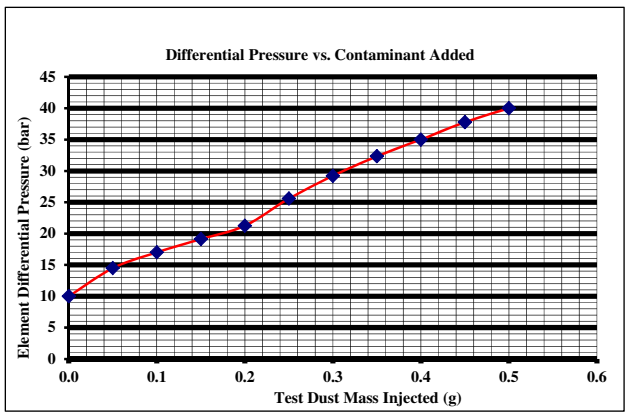

Fig. 10 The differential pressure versus contaminant added graph for pleated part 1V4

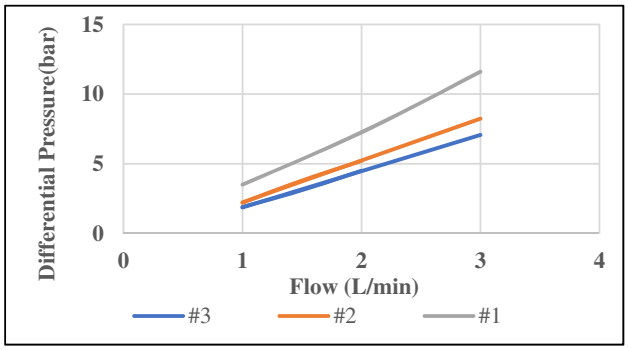

Fig. 11 Flow differential test results of the pleated parts1-3V4

is typical of a metallic filter with very rigid and inflexible pores (Fig. 11).

The differential pressure versus contaminant added curve for conventional fabric filter is closer in appearance to an exponential curve. Initially the rise in differential pressure is slow and steady until the pores are blocked and then it rises rapidly.

Usually during a multi-pass test it is expected for a filter to have reached 50% of its dirt holding capacity when the initial clean differential pressure has doubled.

3.9 Flow versus the Differential pressure test[10, 22]

Another characteristic of a filter including 3D printed metallic filters is the flow versus differential pressure.

There is a direct corelation between the level of porosity or permeability and the pressure drop across the filter. The more porous or coarser a filter the lower is the pressure drop. Likewise, the more the surface area, the lower the pressure drop for a given flow rate.

The initial cylindrical parts were tested at a flow rate of 25 ml/min. To conduct the tests the parts were placed directly between the upstream and downstream particle sensors with a manufacturers flow rate of 25 ml/min.

The larger pleated parts were tested at the minimum low flow circuit of the test facility of 2 L/min. Although this is a low flow rate, it provides a longer test time to accumulate more data for analysis.

Increased test flow rate or dirt holding capacity may be achieved in a number of ways depending on the requirements. This can be achieved by increasing the size of individual parts or increasing the number of units in parallel or in a matrix.

Using SLM and geometrically undefined method of manufacture makes scaling up or down the size or shape of the porous part very easy and convenient without the complexities that would be involved in increasing the size of a lattice or mesh structures for example to maintain the pore sizes consistent.

3.10 Tensile Tests

Figure 12 shows the result of tensile tests carried out on a series of standardised tensile test samples printed out at different energy densities with 2 and 3 mm wall thickness to correspond to cylindrical and pleated part wall thicknesses.

The results show comparable results with those expected of wrought stainless steel material [23].

4 Discussion

From the visual inspections (SEM, X-Ray, Microscopic imaging), fabrication integrity, and multi-pass filtration efficiency test results it is reasonable to conclude that it is perfectly plausible to use ProX DMP 300 to seamlessly manufacture a hybrid porous and fully dense combination products for filtration as well as products for many other industrial, healthcare, and domestic applications where hybrid metallic parts, lighter weight, compact and intricate designs are the required attributes.

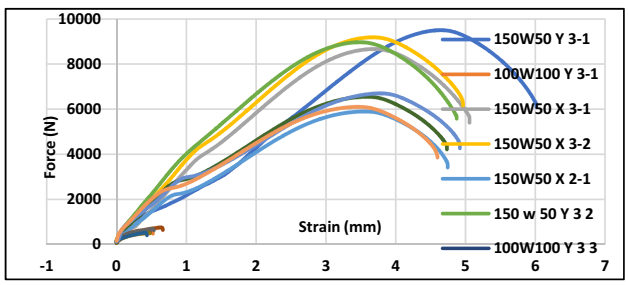

Fig. 12 Tensile testing of standardized porous and solid samples 2 &3 mm thickness

4.1 Cylindrical Parts Summary of Test Results

The summary of the performance of cylindrical parts are tabulated below and it is clear to see the correlation between energy density [24], fabrication integrity, and filtration performance.

4.2 Pleated Parts Summary of Test Results

After the production of porous parts using the Prox 300 DMP and the subsequent fabrication integrity and filtration efficiency testing and reviewing the results, it was concluded that it was feasible to use the DMLS technique and ProX MDP 300 to make metallic permeable media with good physical properties.

The printed pleated porous parts were pressure tested in both forward and reverse flow directions. In an out-in direction up to 40 bar differential pressure and in–out (reverse direction) to 30 bar. In both cases, the test was terminated due to reaching the test equipment limits. The actual collapse pressure of porous metal filters is expected to exceed the above values, especially in an out-in direction. This is favourable compared to a typical standard medium-pressure hydraulic filter which commonly has a maximum working pressure of 20 bar.

Given the filtration rating and mechanical strength of the manufactured parts, it can also be concluded that it is feasible to use them in a range of filtration applications such as high strength, high pressure, and cleanable filters, prefilters, and last chance filters.

In Tables 8 and 9 it can be seen how volumetric energy density influences permeability hence filtration performance. The bubble point test results expressed in inches of water gauge (“WG) suggests volumetric energy densities less than 15 (J/mm^3) will result in a part that is very permeable and not suitable for manufacturing fine filters. On the opposite side of the spectrum a volumetric energy density of 29 or more will result in a part that is going to be too dense and very fine.

Although the above range may seem like a relatively limited range, the permutation for achieving this range is quite large given the number of variables that contribute to the equation, namely hatch distance, layer thickness, scanning speed and very importantly the laser power.

Table 8 Printing parameters, Bubble test, and Filtration ratio summary for the cylindrical parts

Printing parameters				Bubble test ("WG)		Filtration ratio's size(μm) where ß is		
ID	Laser Power (W)	Hatch Distance (μm)	Energy density (J/mm^3)	1st	Fizz "WG	ß = 2	ß = 10	ß = 75
4	120	160	15.63	6.7	13.4	12.4	23.9	> 40
6	100	100	20.83	5.7	23.5	5.11	14.27	> 40
7	100	130	16.03	4.3	7.9	14	> 40	> 40

Table 9 Printing parameters, Bubble test, and Filtration ratio summary for the pleated samples

	Printing parameters		Bubble test results ("WD)		Filtration ratio's size(μm) where ß =			
ID	Hatch Distance (μm)	Energy density* (J/mm^3)	1st	fizz	ß = 2	ß = 10	ß = 75	ß = 100
1V1	80	26.04	6.1	17.2	< 4	27.5	> 40	> 40
2V1	100	20.83	5.2	8.7	22.5	38.5	> 40	> 40
1V2	80	26.04	12.3	64.9	< 4	21.1	34.7	36.7
1V4	75	27.78	29.1	100 +	< 4	25.5	37.3	38.2
3V4	85	24.51	10.1	76.4	< 4	24.9	39.2	> 40

*Laser power was 100W throughout for the above

From Table 9 filtration ratio's summary for the pleated parts, it can also be seen parts 1V2 and 1V4 gave a filtration ratio's of ß = 100 at 36.7 μm and 38.2 μm respectively. The ß ratio which is the industry standard representation of filter efficiency simply notes that for parts 1V2 and 1V4 for every 100 particles of 36.7 μm and 38.2 μm respectively present upstream of the filter only 1 escape downstream. In another word the filter is 99% efficient. It should be born in mind that there is a trade off between the level of the cleanliness that is achieved by a filter and the dirt holding capacity or in another word the useful life of a filter. The finer the filter the more contaminant is captured and the more quickly the filter is blocked and the more quickly the differential pressure across the filter reaches the specified maximum limit. At this point a conventional filter is changed with a new one.

5 Conclusion

The introduction of a general-purpose, high-strength, metallic filter that is compatible with a wide range of operating conditions, process fluids, system pressures, and temperatures that is also cleanable will ultimately lead to reduced cost to both manufacturers and consumers and the reduce demand for new raw materials, reduced energy usage and less pollution.

Various types of filters are used in industries and the domestic markets across the world. Filters are used in industries including manufacturing, aerospace, food and beverages, water purification, medical, and pharmaceutical to name but a few. When filters reach the end of their useful life they are discarded and very often as hazardous waste. A metallic filter that may be cleaned and reused can potentially save money, energy, and consequently reduce pollution. They are therefore environmentally friendly, will have a very long service life and recyclable if required. Using the fusion bed technique to manufacture permeable metallic filter medium with geometrically undefined pores makes it possible to design them conveniently to virtually any shape, a wide range of sizes within the range of equipment used and geometry for many industrial applications. At the same time, it is possible to incorporate them into a fully solid section in the form of a filtration housing for example, add additional support, and strengthening structures all in one operation. They are easily scalable and can be incorporated into complete filtration systems to self-clean and monitor the system conditions and process parameters. As a result, they may be deployed in remote places with minimal human intervention and supervision.

There is also ample scope for improving the product performance in many respects which, due to the time and resources constraints was not possible at this time.

Funding The funding for this research was provided through sponsorship of Mr. S H Haiati on a PhD research course at the University of Portsmouth by the author's employer in UK, Pall Corporation, Portsmouth, UK.

Data Availability Test data is available on a separate spreadsheet.

Declarations

Ethical screening statement This article details a section of primarily laboratory-based scientific research. The research did not involve personal data, human or animal experimentation and therefore does not raise any related ethical issues. The study was conducted in accordance with the University of Portsmouth code of practice, and the research was approved by the Ethics Committee of 2021 Ref: (ETHICS 10283).

References

1. Metal 3D printer. Available from: https://www.3dsystems.com/3d-printers/metal
2. Alomarah, A., Zhang, J., Ruan, D., Masood, S., & Lu, G. Mechanical properties of the 2D re-entrant honeycomb made via direct metal printing. *IOP Conference Series: Materials Science and Engineering*.
3. DMLS 3D printing: Metal manufacturing at its best. Available from: https://www.eos.info/en/additive-manufacturing/dmls
4. Nandy, J., Sarangi, H., & Sahoo, S. (2019). A review on direct metal laser sintering: process features and microstructure modeling. *Lasers in Manufacturing and Materials Processing, 6*, 280–316. https://doi.org/10.1007/s40516-019-00094-y
5. Kruth, J., Van der Schueren, B., Bonse, J., & Morren, B. (1996). Basic powder metallurgical aspects in selective metal powder sintering. *CIRP Annals, 45*(1), 183–186. https://doi.org/10.1016/S0007-8506(07)63043-1
6. Van der Schueren, B., Kruth, J. P. (1994). Laser based selective metal powder sintering: a feasibility study. In *Proceedings of the Laser Assisted Net Shape Engineering*, pp. 517–523.
7. Industrial metal AM machines. Available from: https://www.slm-solutions.com/products-and-solutions/machines/
8. Liu, Y., Yang, Y., & Wang, D. (2016). A study on the residual stress during selective laser melting (SLM) of metallic powder. *International Journal of Advanced Manufacturing Technology, 87*, 647–656. https://doi.org/10.1007/s00170-016-8466-y
9. Jafari, D., Wits, W. W., Vaneker, T. H., Demir, A. G., Previtali, B., Geurts, B. J., & Gibson, I. (2020). Pulsed mode selective laser melting of porous structures: Structural and thermophysical characterization. *Additive Manufacturing, 35*, 101263. https://doi.org/10.1016/j.addma.2020.101263
10. Ma, S., Tang, Q., Han, X., Feng, Q., Song, J., Setchi, R., Liu, Y., Liu, Y., Goulas, A., Engstrøm, D. S., Tse, Y. Y., & Zhen, N. (2020). Manufacturability, mechanical properties, mass-transport properties and biocompatibility of triply periodic minimal surface (TPMS) porous scaffolds fabricated by selective laser melting. *Materials & Design, 195*, 109034. https://doi.org/10.1016/j.matdes.2020.109034
11. Hall, E. L., Dietrich, A. M. (2000). A brief history of drinking water. *Opflow*, *26*(6), 46–49. https://doi.org/10.1002/j.1551-8701.2000.tb02243.x. https://www.researchgate.net/publication/325781903_A_Brief_History_of_Drinking_Water
12. Xu Z. (2013). Filtration mechanism of fine particle. Fundamentals of air cleaning technology and its application in cleanrooms. 133–183. https://doi.org/10.1007/978-3-642-39374-7_3
13. Guddati, S., Kiran, A. S. K., Leavy, M., et al. (2019). Recent advancements in additive manufacturing technologies for porous material applications. *International Journal of Advanced Manufacturing Technology, 105*, 193–215. https://doi.org/10.1007/s00170-019-04116-z
14. Płatek, P., Sienkiewicz, J., Janiszewski, J., & Jiang, F. (2020). Investigations on mechanical properties of lattice structures with different values of relative density made from 316L by selective laser melting (SLM). *Materials, 13*(9), 2204. https://doi.org/10.3390/ma13092204
15. ISO 2942:2018- Hydraulic fluid power. Filter elements. Verification of fabrication integrity and determination of the first bubble point
16. ISO 16889:2022- Hydraulic fluid power — Filters — Multi-pass method for evaluating filtration performance of a filter element
17 Zhu, B., Duke, M., Dumée, L. F., Merenda, A., Des Ligneris, E., Kong, L., Hodgson, P. D., & Gray, S. (2018). Short review on porous metal membranes—fabrication, commercial products, and applications. *Membranes, 8*, 83. https://doi.org/10.3390/membranes8030083
18. Singh, H., Saxena, P., & Puri, Y. (2021). The manufacturing and applications of the porous metal membranes: A critical review. *CIRP Journal of Manufacturing Science and Technology, 33*, 339–368. https://doi.org/10.1016/j.cirpj.2021.03.014
19. Furumoto, T., Koizumi, A., Alkahari, M. R., Anayama, R., Hosokawa, A., Tanaka, R., & Ueda, T. (2015). Permeability and strength of a porous metal structure fabricated by additive manufacturing. *Journal of Materials Processing Technology, 219*, 10–16. https://doi.org/10.1016/j.jmatprotec.2014.11.043
20. Hanninen, J. Direct metal laser sintering: Direct metal laser sintering (DMLS) is an advanced rapid tooling and manufacturing process that enables production of true net-shape metal parts directly from three-dimensional CAD data. *Advanced Materials & Processes*, *160*(5).
21. Laser form 17–4PH datasheet. Available from: https://www.3dsystems.com/materials/laserform-17-4ph
22. ISO 3968:2017(en), Hydraulic fluid power — filters — evaluation of differential pressure versus flow.
23. Ponnusamy, P., Sharma, B., Masood, S., Rahman Rashid, R., Rashid, R., Palanisamy, S., & Ruan, D. (2021). A study of tensile behavior of SLM processed 17–4 PH stainless steel. *Materials Today: Proceedings, 45*, 4531–4534. https://doi.org/10.1016/j.matpr.2020.12.1104
24. Xie, D., & Dittmeyer, R. (2021). Correlations of laser scanning parameters and porous structure properties of permeable materials made by laser-beam powder-bed fusion. *Additive Manufacturing, 47*, 102261. https://doi.org/10.1016/j.addma.2021.102261

Seyed Hessamedin Haiati is an engineer working in the liquid qualification laboratory for Pall Europe in Portsmouth, United Kingdom. He specializes in development of filter test stands, construction of bespoke test rigs, testing and writing of test procedures. He has extensive knowledge of hydraulic and pneumatic systems as well as a working knowledge of electrical engineering and a wide range of testing and analysis software. Hessam has obtained a postgraduate diploma in Integrated Electronic Product Design and an MSc in Product Engineering. Hessam is currently studying for a PhD at University of Portsmouth.

Dr Krassimir Dotchev is a Senior Lecturer in Mechanical Engineering and CAD/CAM in the School of Mechanical and Design Engineering, University of Portsmouth. His academic and research interests encompass the areas of CAD/CAM in Mechanical Engineering, Product Design, and Additive Manufacturing. He was a team leader in many research and industrial projects in the area of engineering design, rapid product development and manufacturing. Dr Dotchev has more than 20 years' experience with CAD/CAM as essential enabling technologies in engineering design. He holds a PhD and Dipl. Eng. in Mechanical Engineering. Dr Dotchev is a Chartered Engineer, a Member of the Institution of Engineering and Technology (IET) and a Fellow of the Higher Education Academy. He has published more than 50 technical papers in journals and conference proceedings.

Morgan Lowther is an adaptable researcher with a history of working in industrial R&D. He has hands-on industrial experience of the entire Additive Manufacturing process chain, from powder to final product. Morgan Lowther won The Young Persons' Lecture Competition in the Institute of Minerals, Mining and Materials (IOM3) when he was a PhD student at the University of Birmingham Healthcare Technologies Institute. Morgan was later part of a team from The University of Portsmouth who constructed a 3D model of the skull of a victim when he was working as a Senior Scientific Officer in The Future Technology Laboratory. The skull was used in a trial that concluded with the conviction of four individuals.